ChemComm

Check for updates

A supramolecular porous material comprising Fe(II) mesocates†

Benjamin H. Wilson,[a] Hayley S. Scott,[a] Omid T. Qazvini,[b] Shane G. Telfer, [iD] [b] Corine Mathonière,[cd] Rodolphe Clérac [iD] [ef] and Paul E. Kruger [iD] *[a]

The dinuclear mesocate [Fe₂L₃](BF₄)₄, 1, is a supramolecular building block for a microporous material. Structural analysis reveals that extensive noncovalent interactions in the solid state generate a 3D framework with microporous channels. These channels are permanently accessible to incoming guest molecules and adsorption isotherms demonstrate that the material has a high selectivity for CO_2 over N_2.

Over the past two decades, our understanding of microporous materials has progressed, steadily driven by their relevance to diverse applications such as gas separation and storage, catalysis, small-molecule separation and chemical sensing.[1] 3D polymeric architectures, sustained by covalent and metal–ligand interactions, comprise the majority of microporous materials that have uniform and periodic structures. Notably, these include naturally occurring zeolites,[2] metal–organic-frameworks (MOFs)[3] and covalent-organic-frameworks (COFs).[4] More recently, however, an increasing number of studies have been devoted to porous materials comprised of discrete molecular entities.[5] This class of compound, called molecular porous materials (MPMs),[6] offer synthetic advantages over 3D polymeric materials owing to their enhanced solubility, which may aid their processability and incorporation into functional materials (*e.g.* attachment to surfaces, *etc.*). Two broad classes, depending on their structural conformation, describe the porosity within MPMs. Intrinsic porosity refers to compounds in which accessible void space is found inside a discrete entity *e.g.* organic cages,[7]

metal–organic-squares (MOSs)[8] and polyhedra (MOPs)[9] *etc.* Extrinsic porosity refers to structures in which void space exists between molecular units. Because the packing density in conventional molecule-based solids is high, the formation of MPMs possessing extrinsic porosity is rare. However, a reduction of the packing density *via* constructive and supportive supramolecular interactions between molecules can realise porous architectures. These supramolecular interactions typically involve hydrogen bonding, as in hydrogen-bonded organic frameworks (HOFs),[10] supramolecular metal–organic frameworks (SMOFs),[11] and supramolecular organic frameworks (SOFs),[12] or noncovalent interactions involving strong dipoles.[5a,12] There is much to learn from new examples of extrinsically porous materials, in particular the relationship between structural features and their properties, including stability, permanent porosity and solubility.

As part of our programme investigating Fe(II) dinuclear complexes[13] (Fig. 1), we report here a new and rare example of an extrinsically porous material comprising a supramolecular building block. The compound, [Fe₂L₃](BF₄)₄, 1, where L = *N,N*-3-bis[1-(2-pyrazinyl)ethylidene]isophthalo-hydrazide, was characterised using single crystal X-ray diffraction, and its permanent porosity was evaluated by gas adsorption isotherms using a range of adsorbates.
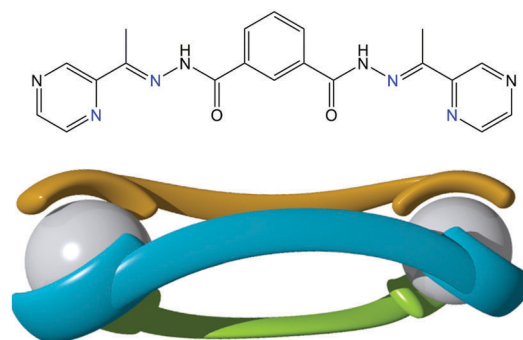
[a] *MacDiarmid Institute for Advanced Materials and Nanotechnology, School of Physical and Chemical Sciences, University of Canterbury, Private Bag 4800, Christchurch 8041, New Zealand. E-mail: paul.kruger@canterbury.ac.nz*

[b] *MacDiarmid Institute for Advanced Materials and Nanotechnology, Institute of Fundamental Sciences, Massey University, Palmerston North 4442, New Zealand*

[c] *CNRS, ICMCB, UMR 5026, F-33600 Pessac, France*

[d] *Univ. Bordeaux, ICMCB, UMR 5026, F-33600 Pessac, France*

[e] *CNRS, CRPP, UMR 5031, F-33600 Pessac, France*

[f] *Univ. Bordeaux, CRPP, UMR 5031, F-33600 Pessac, France*

Fig. 1 (top) Structure of the ligand, **L**, used in the current study with coordinating N-atoms coloured blue. (bottom) Schematic of a dinuclear triply stranded mesocate of composition $[M_2L_3]^{n+}$.
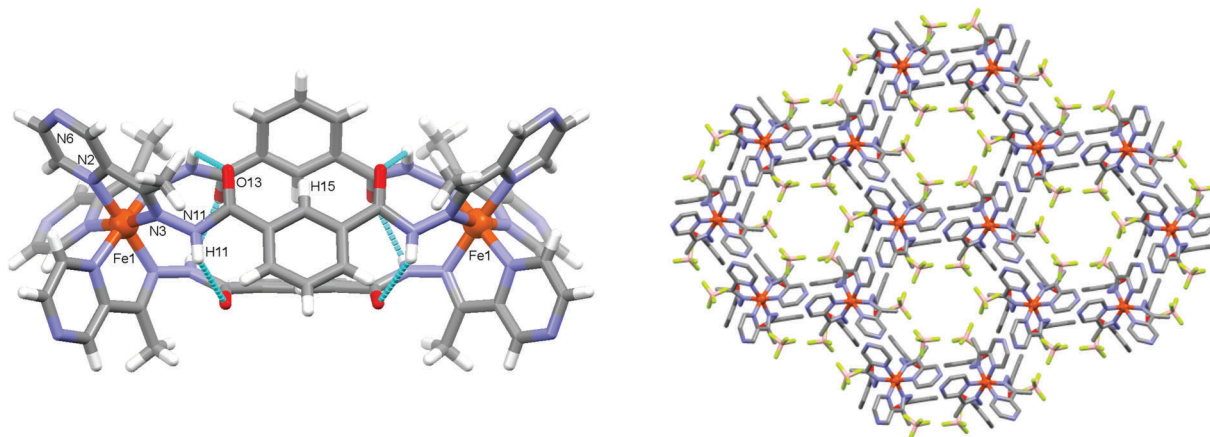
Fig. 2 (left) Molecular and crystal structure of the dinuclear mesocate complex, **1**. Anions and disordered solvate molecules removed for clarity. (right) Packing diagram of **1** view down the crystallographic *c*-axis. H-atoms and disordered solvate molecules omitted for clarity.

A red coloured solution resulted when a suspension of **L** in nitromethane was stirred with $Fe(BF_4)_2$ (2 : 3) at room temperature overnight. Single crystals of **1** were obtained by the diffusion of toluene anti-solvent into the nitromethane solution (see ESI†). The structure of **1** was determined from X-ray diffraction data collected at 120 K. It crystallises in the hexagonal space group $P6_3/m$. The asymmetric unit contains one third of an Fe(II) atom coordinated to half of a ligand fragment featuring bidentate coordination *via* pyrazine (N2) and hydrazide (N3) nitrogen donors (Fig. 2 and Fig. S2, ESI†). The average Fe–N bond length of 1.959(4) Å reveals the Fe(II) centre exists in the low spin state at 120 K.[14] The action of a 3-fold rotoinversion congruent with the crystallographic *c*-axis and a reflection about a mirror plane perpendicular to the crystallographic *c*-axis yields the dinuclear complex, $[Fe_2L_3]^{4+}$ (Fig. 2). The three bis-bidentate ligand strands bridge Fe(II) centres to form a compact mesocate replete with attractive noncovalent inter-strand interactions. The hydrazide oxygen atoms (O13) are twisted with respect to the plane of the central phenyl rings to which they are attached and are in close contact with an adjacent hydrazide group from a neighbouring (inter-strand) ligand, O13···H11(N11), 2.957(3) Å, 125.8°. Likewise, H15 from the central phenyl rings participate in an edge-to-face C–H···π interaction with an adjacent ligand strand, C15–H15···π(centre-of-ring) 2.903 Å, 149.6° (Fig. 2, Fig. S3; Tables S2, S3, ESI†). These interactions likely support the mesocate conformation.

The mesocates pack in the crystal lattice *via* extensive supramolecular interactions, the most salient of which is the hydrogen-bonding between pyrazine and hydrazide groups of adjacent mesocates *e.g.* N11–H11···N6, 3.009(8) Å, (Fig. S4, ESI†). There are six (reciprocal) hydrogen bonds between adjacent pyrazine and hydrazide moieties of neighbouring supra-molecules, along with offset face-to-face π–π interactions involving each pyrazine ring (centroid···centroid, 3.687(3) Å). These interactions propagate down the crystallographic *c*-axis to generate a network containing 1D hexagonal channels parallel with the *c*-axis (Fig. 2, Fig. S4–S7; Tables S2, S3, ESI†). The channel diameter at closest contact between van der Waals surfaces is *ca.* 5.8 Å. The tetrafluoroborate anions (which are disordered over two positions) line these 1D channels. Because of the high symmetry of the space
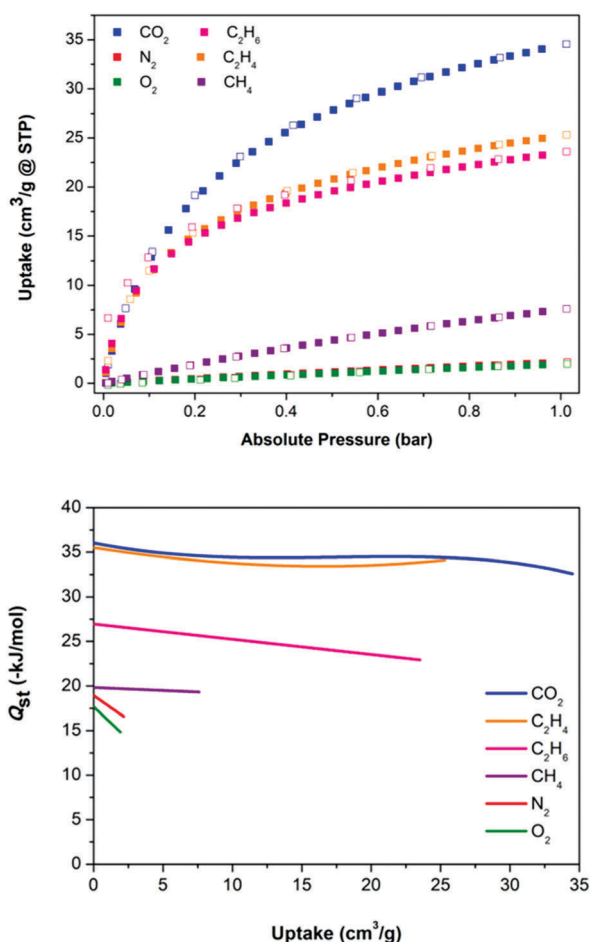

Fig. 3 (top) Adsorption isotherms for **1** at 295 K. (bottom) Plot of Q_{st} as a function of loading for sorbates within **1**.

group and disorder within the solvent molecules that reside within the channels, their identities could not be accurately determined and they were therefore treated by using the *SQUEEZE* programme embedded within *PLATON*.[15] The solvent accessible void was calculated to be 1164 Å³ and accounts for 26% of the crystal volume.

Table 1 Summary of gas sorption results for **1**

Void space[a]	N_2 uptake[b] ($cm^3\ g^{-1}$), Q_{st}[c] ($-kJ\ mol^{-1}$)	CO_2 uptake[b] ($cm^3\ g^{-1}$), Q_{st}[c] ($-kJ\ mol^{-1}$)	CH_4 uptake[b] ($cm^3\ g^{-1}$), Q_{st}[c] ($-kJ\ mol^{-1}$)	C_2H_4 uptake[b] ($cm^3\ g^{-1}$), Q_{st}[c] ($-kJ\ mol^{-1}$)	C_2H_6 uptake[b] ($cm^3\ g^{-1}$), Q_{st}[c] ($-kJ\ mol^{-1}$)	O_2 uptake[b] ($cm^3\ g^{-1}$), Q_{st}[c] ($-kJ\ mol^{-1}$)
26%	2.1, 18.9	34.5, 36.0	7.5, 19.8	25.3, 35.5	23.6, 26.9	1.9, 17.7

[a] The accessible void space and micropore volume were calculated with the program *PLATON*[15] using a probe radius of 1.2 Å. [b] Uptakes reported at 1 bar and 295 K ($cm^3\ g^{-1}$). [c] Sorption data at 273 and 295 K were fit to a virial function from which the isosteric enthalpy of adsorption (Q_{st}, kJ mol^{-1}) was calculated.

Intrigued by the presence and size of the 1D channels within this material, and the structural resilience of the crystals when removed from their mother liquor, we set about to appraise its permanent porosity. Powder X-ray diffraction (PXRD) verified that activation of a batch of crystals *via* solvent exchange and drying *in vacuo* successfully retained the lattice structure (Fig. S8, ESI†). The accessibility of the activated material to incoming guests molecules was confirmed by a H_2 adsorption isotherm at 77 K, which showed an uptake in excess of 60 $cm^3\ g^{-1}$ (Fig. S9, ESI†). Hysteresis is also evident in this isotherm and is most probably a consequence of the small size of the pores and their one dimensional nature, which leads to slow diffusion of H_2 at 77 K. Consistent with the small size of the 1D channels, the uptake of N_2 at 77 K was hampered by slow diffusion kinetics, which precluded the measurement of a conventional BET surface area. Gas uptake around room temperature was unhindered, however, and adsorption isotherms at 273 and 295 K were measured for the adsorbates CO_2, O_2, N_2, CH_4, C_2H_4 and C_2H_6 (Fig. 3, Table 1 and Fig. S14, ESI†). The small hysteresis in the 295 K isotherms for ethane possibly arises as a consequence of its larger size and indicates that we are approaching the size limit of the guests that can be adsorbed into the small 1D channels in **1**.

From the range of adsorbates tested, the uptakes of CO_2 and N_2 are striking (Table 1). They reveal a significant uptake of CO_2 and very little of N_2: at 295 K and 1 bar, uptake capacities of CO_2 and N_2 are equal to 34.5 and 2.1 $cm^3\ g^{-1}$, respectively. This behaviour is a highly desirable feature touted for materials used in CO_2 removal from flue gas streams and has been observed in other microporous physisorbent materials.[16,17] The selectivity for CO_2 over N_2 in a 1:1 mixture was calculated using IAST to vary between 75 (low pressure) and 40 (1 bar), as shown in Fig. S25 (ESI†). The selectivity of **1** for this gas pair is higher than those reported for a number of well-known MOFs, including CuBTC,[18] SIFSIX-1-Cu[6b] and PCN-61.[19] The selectivity for CO_2 over methane is also impressive, varying between 16 and 20 (Fig. S25, ESI†). Breakthrough curves for these gas pairs were simulated. These predict that **1** has the clear potential to separate CO_2/N_2 and CO_2/CH_4 mixtures on a bulk scale.

To evaluate the strength of interactions between adsorbates and **1**, their isosteric heats of adsorption (Q_{st}) were calculated (Fig. 3 and Fig. S11–S23, ESI†). For the six adsorbates, the magnitude of the Q_{st} values follow the same trend of the uptake capacities (Table 1). Notably, for CO_2 the enthalpy at low loading is equal to 36 kJ mol^{-1}, and for N_2 19 kJ mol^{-1}. These values are on par with expectations based on the quadrupole moments and polarisabilities of these adsorbates, and are comparable with values observed for MOFs and related porous materials.[20] Notably, the Q_{st} for N_2 is higher than that of O_2.

This is the reverse of that expected on the basis of van der Waals interactions and is due to the quadrupole moment of N_2 and its interaction with the strong electric field gradient of **1** that stems from the presence of the BF_4^- anions in the channels. A similar situation is seen in zeolites, which are also highly polar. For MOFs the situation is usually the reverse ($O_2 > N_2$) since their pores are typically less polar.

In conclusion, a new molecular porous material constructed from dinuclear mesocate complexes $[Fe_2(L)_3](BF_4)_4$, **1**, has been detailed and represents a rare example of an extrinsically porous material. The formation of extensive supramolecular interactions between mesocate complexes serve to sustain an overall 3D architecture. 1D channels protruding through the structure have been studied by gas sorption experiments and reveal high CO_2 over N_2 selectivity, surpassing several well-known MOFs. These results serve to emphasise the advantages offered by MPMs for selective gas sorption and provide design strategies for establishing new variants. Current work in our laboratory is looking at new variants of compound **1** by using related ligand sets in combination with other metal salts and results from these studies will be reported in due course.

Conflicts of interest

There are no conflicts to declare.

Notes and references

1 (a) F. Rouquerol, J. Roquerol, D. S. W. Sing, P. Llewellyn and G. Maurin, *Adsorption by Powders and Porous Solids: Principles, Methodology and Applications*, Elsevier, Poland, 2nd edn, 2014; (b) P. A. Wright, *Microporous Framework Solids*, Royal Society of Chemistry, Cambridge, 2008; (c) H. Yang, S. J. Bradley, X. Wu, A. Chan, G. I. N. Waterhouse, T. Nann, J. Zhang, P. E. Kruger, S. Ma and S. G. Telfer, *ACS Nano*, 2018, **12**, 4594; (d) H. Yang, S. J. Bradley, A. Chan, G. I. N. Waterhouse, T. Nann, P. E. Kruger and S. G. Telfer, *J. Am. Chem. Soc.*, 2016, **138**, 11872.

2 R. Xu, W. Pang, J. Yu, Q. Huo and J. Chen, *Chemistry of Zeolites and Related Porous Materials: Synthesis and Structure*, John Wiley & Sons Ltd, Singapore, 2007.

3 (*a*) *Metal-Organic Framework Materials*, ed. C. M. Lukehart and L. R. MacGillivray, John Wiley & Sons Ltd, United Kingdom, 2014; (*b*) *The Chemistry of Metal-Organic Frameworks: Synthesis, Characterization, and Applications*, ed S. Kaskel, Wiley-VCH Verlag GmbH & Co., 2016; (*c*) D. C. Young, H. Yang, S. G. Telfer and P. E. Kruger, *Inorg. Chem.*, 2017, **56**, 12224; (*d*) H. S. Scott, S. Mukherjee, D. R. Turner, M. I. J. Polson, M. J. Zaworotko and P. E. Kruger, *CrystEngComm*, 2018, **20**, 1193; (*e*) S. J. Lee, C. Doussot and S. G. Telfer, *Cryst. Growth Des.*, 2017, **17**, 3185; (*f*) K. M. Patil, S. G. Telfer, S. C. Moratti, O. T. Qazvini and L. R. Hanton, *CrystEngComm*, 2017, **19**, 7236.

4 S.-Y. Ding and W. Wang, *Chem. Soc. Rev.*, 2013, **42**, 538.

5 (*a*) N. B. McKeown, *J. Mater. Chem.*, 2010, **20**, 10588; (*b*) J. Tian, P. K. Thallapally and B. P. McGrail, *CrystEngComm*, 2012, **14**, 1909; (*c*) A. G. Slater and A. I. Cooper, *Science*, 2015, **348**, 6238; (*d*) C. G. Bezzu, M. Helliwell, J. E. Warren, D. R. Allan and N. B. McKeown, *Science*, 2010, **327**, 1627.

6 (*a*) H. Kim, Y. Kim, M. Yoon, S. Lim, S. M. Park, G. Seo and K. Kim, *J. Am. Chem. Soc.*, 2010, **132**, 12200; (*b*) P. S. Nugent, V. L. Rhodus, T. Pham, K. Forrest, L. Wojtas, B. Space and M. J. Zaworotko, *J. Am. Chem. Soc.*, 2013, **135**, 10950.

7 T. Tozawa, J. T. A. Jones, S. I. Swamy, S. Jiang, D. J. Adams, S. Shakespeare, R. Clowes, D. Bradshaw, T. Hasell, S. Y. Chong, C. Tang, S. Thompson, J. Parker, A. Trewin, J. Bacsa, A. M. Z. Slawin, A. Steiner and A. I. Cooper, *Nat. Mater.*, 2009, **8**, 973.

8 S. Wang, T. Zhao, G. Li, L. Wojtas, Q. Huo, M. Eddaoudi and Y. Liu, *J. Am. Chem. Soc.*, 2010, **132**, 18038.

9 (*a*) A. C. Sudik, A. R. Millward, N. W. Ockwig, A. P. Côté, J. Kim and O. M. Yaghi, *J. Am. Chem. Soc.*, 2005, **127**, 7110; (*b*) M. B. Duriska, S. M. Neville, J. Lu, S. S. Iremonger, J. F. Boas, C. J. Kepert and S. R. Batten, *Angew. Chem., Int. Ed.*, 2009, **121**, 9081; (*c*) G. A. Craig, P. Larpent, S. Kusaka, R. Matsuda, S. Kitagawa and S. Furukawa, *Chem. Sci.*, 2018, **9**, 6463; (*d*) J.-R. Li and H.-C. Zhou, *Nat. Chem.*, 2010, **2**, 893; (*e*) W. Lu, D. Yuan, A. Yakovenko and H.-C. Zhou, *Chem. Commun.*, 2011, **47**, 4968; (*f*) J. M. Teo, C. J. Coghlan, J. D. Evans, E. Tsivion, M. Head-Gordon, C. J. Sumby and C. J. Doonan, *Chem. Commun.*, 2016, **52**, 276; (*g*) K. Xiong, F. Jiang, Y. Gai, D. Yuan, L. Chen, M. Wu, K. Su and M. Hong, *Chem. Sci.*, 2012,

3, 2321; (*h*) D. Preston, K. F. White, J. E. M. Lewis, R. A. S. Vasdev, B. F. Abrahams and J. D. Crowley, *Chem. – Eur. J.*, 2017, **23**, 10559.

10 H. Wang, B. Li, H. Wu, T.-L. Hu, Z. Yao, W. Zhou, S. Xiang and B. Chen, *J. Am. Chem. Soc.*, 2015, **137**, 9963.

11 J. Thomas-Gipson, G. Beobide, O. Castillo, M. Fröba, F. Hoffmann, A. Luque, S. Pérez-Yáñez and P. Román, *Cryst. Growth Des.*, 2014, **14**, 4019.

12 J. Tian, H. Wang, D.-W. Zhang, Y. Liu and Z.-T. Li, *Natl. Sci. Rev.*, 2017, **4**, 426.

13 (*a*) R. J. Archer, C. S. Hawes, G. N. L. Jameson, V. McKee, B. Moubaraki, N. F. Chilton, K. S. Murray, W. Schmitt and P. E. Kruger, *Dalton Trans.*, 2011, **40**, 12368; (*b*) D. Pelleteret, R. Clérac, C. Mathonière, E. Harté, W. Schmitt and P. E. Kruger, *Chem. Commun.*, 2009, 221; (*c*) R. J. Archer, H. S. Scott, M. I. J. Polson, B. E. Williamson, C. Mathonière, M. Rouzières, R. Clérac and P. E. Kruger, *Dalton Trans.*, 2018, **47**, 7965.

14 Single crystal X-ray diffraction data were also collected at 298 K. While the quality of the crystal was poor, the data gave a reasonable structural solution in the same $P6_3/m$ space group. The average Fe–N bond length of 1.958(10) Å reveals that the Fe(II) centre remains in the low spin state at 298 K.

15 A. L. Spek, PLATON SQUEEZE: a tool for the calculation of the disordered solvent contribution to the calculated structure factors, *Acta Crystallogr., Sect. C: Cryst. Struct. Commun.*, 2015, **71**, 9.

16 D. Aaron and C. Tsouris, *Sep. Sci. Technol.*, 2005, **40**, 321.

17 (*a*) J. Thomas-Gipson, G. Beobide, O. Castillo, J. Cepeda, A. Luque, S. Pérez-Yáñez, A. T. Aguayo and P. Román, *CrystEngComm*, 2011, **13**, 3301; (*b*) K. M. Ok, J. Sung, G. Hu, R. M. J. Jacobs and D. O'Hare, *J. Am. Chem. Soc.*, 2008, **130**, 3762; (*c*) T. K. Maji, R. Matsuda and S. Kitagawa, *Nat. Mater.*, 2007, **6**, 142.

18 Z. Zhang, Y. Zhao, Q. Gong, Z. Lib and J. Li, *Chem. Commun.*, 2013, **49**, 653.

19 B. Zheng, J. Bai, J. Duan, L. Wojtas and M. J. Zaworotko, *J. Am. Chem. Soc.*, 2011, **133**, 748.

20 (*a*) H. S. Scott, N. Ogiwara, K.-J. Chen, D. G. Madden, T. Pham, K. Forrest, B. Space, S. Horike, J. J. Perry, S. Kitagawa and M. J. Zaworotko, *Chem. Sci.*, 2016, **7**, 5470; (*b*) K.-J. Chen, H. S. Scott, D. G. Madden, T. Pham, A. Kumar, A. Bajpai, M. Lusi, K. A. Forrest, B. Space, J. J. Perry and M. J. Zaworotko, *Chem*, 2016, **1**, 753; (*c*) P. Nugent, Y. Belmabkhout, S. D. Burd, A. J. Cairns, R. Luebke, K. Forrest, T. Pham, S. Ma, B. Space, L. Wojtas, M. Eddaoudi and M. J. Zaworotko, *Nature*, 2013, **495**, 80.